Aspect Differences in Vegetation Type Drive Higher Evapotranspiration on a Pole-facing Slope in a California Oak Savanna

Amanda Donaldson[1*], David Dralle[2], Nerissa Barling[1], Russell Callahan[1,3], Michael E. Loik[4], Margaret Zimmer[1,5]

[1]Department of Earth and Planetary Sciences, University of California, Santa Cruz, CA, USA.

[2]Pacific Southwest Research Station, United States Forest Service, Albany, CA, USA.

[3]Department of Earth Sciences, University of Connecticut, Storrs, CT, USA.

[4]Department of Environmental Studies, University of California, Santa Cruz, CA, USA.

[5]U.S. Geological Survey Upper Midwest Water Science Center, Madison, WI, USA.

*corresponding author: amdonald@ucsc.edu

Keywords: evapotranspiration, aspect, soil moisture, remote sensing, oak savanna

Key Points:

- Higher evapotranspiration on cooler pole-facing slope than warmer equator-facing slope within an oak savanna in a Mediterranean climate.
- Aspect-differences in plant functional groups and phenology drive observed evapotranspiration variability.
- Higher evapotranspiration contributes to a drier subsurface on pole-facing slopes.

Abstract

Quantifying evapotranspiration is critical to accurately predict vegetation health, groundwater recharge, and streamflow generation. Hillslope aspect, the direction a hillslope faces, results in variable incoming solar radiation and subsequent vegetation water use that influence the timing and magnitude of evapotranspiration. Previous work in forested landscapes has shown that equator-facing slopes have higher evapotranspiration due to more direct solar radiation and higher evaporative demand. However, it remains unclear how differences in vegetation type (i.e., grasses and trees) influence evapotranspiration and water partitioning between hillslopes with opposing aspects. Here, we quantified evapotranspiration and subsurface water storage deficits between a pole- and equator-facing hillslope with contrasting vegetation types within central coastal California. Our results suggest that cooler pole-facing slopes with oak trees have higher evapotranspiration than warmer equator-facing slopes with grasses, which is counter to previous work in landscapes with singular vegetation types. Our water storage deficit calculations indicate that the pole-facing slope has a higher subsurface storage deficit and a larger seasonal dry down than the equator-facing slope. This aspect difference in subsurface water storage deficits may influence subsequent deep groundwater recharge and streamflow generation. In addition, larger root-zone storage deficits on pole-facing slopes may reduce their ability to serve as hydrologic refugia for oaks during periods of extended drought. This research provides a novel integration of field-based and remotely-sensed estimates of evapotranspiration required to properly quantify hillslope-scale water balances. These findings emphasize the importance of resolving hillslope-scale vegetation structure within Earth system models, especially in landscapes with diverse vegetation types.

Plain Language Summary

Understanding how much water leaves hillslopes as evapotranspiration (i.e. evaporation and plant water use) is important for predicting water storage and movement within hillslopes. Small differences in solar radiation between adjacent hillslopes that face opposite directions can produce contrasting plant water use and hillslope water storage patterns. However, previous studies have focused on landscapes with trees on either hillslope. It remains unclear how the combination of differences of solar radiation and plant type (i.e. grasses and trees) influence evapotranspiration and water storage within hillslopes that face opposite directions. Here, we combined on-site measurements and remote-sensing data to show that in central coastal California, a hillslope with oak trees that received less direct sunlight had higher evapotranspiration than a hillslope with grasses that received more direct sunlight. Importantly, we suggest that the cooler hillslope with oak trees may be drier and have lower groundwater recharge than the warmer hillslope with grasses, which is opposite the findings of studies with trees on both hillslopes. Our findings highlight the critical need for forest managers and modelers to consider hillslope-scale vegetation types to more accurately predict groundwater recharge, streamflow generation, and vegetation health within oak savannas.

1 Introduction

Differences in hillslope aspect, or the direction a hillslope faces, produce subcatchment-scale variability in the delivery of solar radiation to the land surface, which is one of the strongest controls on vegetation distribution and water partitioning within terrestrial landscapes (Chorover et al., 2011; Ying et al., 2019). Equator-facing slopes (EFS; south-facing in the

northern hemisphere) with more direct solar radiation have higher air temperature, aridity, and evaporative demand compared to pole-facing slopes (PFS, north-facing in the northern hemisphere; Smith & Bookhagen, 2021). Current conceptual frameworks depict warmer EFS with higher potential evapotranspiration and subsequently lower infiltration, groundwater recharge, and runoff (García-Gamero et al., 2021; Pelletier et al., 2018; Regmi et al., 2019; Webb et al., 2023). In contrast, cooler PFS are considered to have lower potential evapotranspiration and higher infiltration, groundwater recharge, and runoff (García-Gamero et al., 2021; Pelletier et al., 2018; Regmi et al., 2019; Webb et al., 2023). While this current conceptual model may provide insight into how differences in energy inputs drive hydrologic partitioning, it is unclear if the expected patterns are universal across diverse environments and vegetation types (Brooks et al., 2015; Ying et al., 2019; Zapata-Rios et al., 2016).

Understanding the compounding role of variable solar radiation and plant functional groups (e.g., grass, tree, shrub) is important for determining the transferability of current expectations of hydrologic partitioning between hillslopes with opposing aspects (Kumari et al., 2020). The current conceptual model of hydrologic partitioning within aspect-regulated landscapes is largely based on environments where potential differences in actual evapotranspiration (ET) due to variability in plant functional groups are not incorporated (Pelletier et al., 2018; Regmi et al., 2019). Studies in watersheds with similar plant functional groups (e.g., trees) have shown higher transpiration rates on EFS compared to PFS (Bilir et al., 2021; Burns et al., 2023; Holst et al., 2010). However, there is also documented diversity in the responses of different plant functional groups and species between aspects, which create complex patterns of vegetation water uptake (e.g. due to differences in rooting depth) and have lesser known consequences on subsurface water cycling (Armesto & Martínez, 1978; Gutiérrez-Jurado et al., 2013; Hassler et al., 2018). Given the importance of vegetation water uptake in driving subsurface hydrologic partitioning, understanding the role of vegetation type is required to accurately forecast water cycling patterns within Earth system models (Kumari et al., 2020; Marston et al., 2022; Ying et al., 2019).

Here, we address these knowledge gaps by quantifying hourly to monthly ET and shallow subsurface water storage between a grass-dominated EFS and an oak tree-dominated PFS in central California. We combined field-based measurements of soil moisture, oak and grass transpiration, tree survey-based scaling, and remotely-sensed normalized difference vegetation index (NDVI) and ET to determine how hydrologic partitioning differs between hillslopes with opposing aspects and different plant community types.

2 Methods

2.1 Site Description and Instrumentation

The study site (Arbor Creek Experimental Catchment; 37.393, −121.723) ranges from 720 - 790 m above sea level and is located within the University of California Blue Oak Ranch Reserve (Figure 1). This reserve is located within the Mt. Diablo Range, ~24 km northeast of San Jose, California, USA. The local climate is classified as Mediterranean, with hot, dry summers and cool, wet winters and an average 600 mm of precipitation mostly falling as rain between October - April (Donaldson et al., 2023). Soils are loamy and thin (~50 cm) and the dominant rock types are sandstone and shale consistent with the Yolla Bolly Unit and the Great Valley Sequence (Donaldson et al., 2023).

We installed a weather station (ClimaVUE50, Campbell Scientific; Logan, Utah) at the ridge of the PFS to record precipitation at 10-min intervals from October 1, 2020 - September 30,

2021 (2021 water year). We excavated soil pits at each landscape position (e.g. toeslope, mid-slope, and shoulder) on the PFS and EFS (Figure 1). We monitored soil moisture (ECHO/EC-5, Decagon, Devices Inc. Washington, USA) every 10-min at 10 cm and 50 cm depths from winter 2020 through September 2021(start date varied due to sensor installation).

The study site is characterized as a mixed-deciduous oak savanna composed of blue oak (*Quercus douglasii* Hook., Fagaceae), black oak (*Quercus kelloggii*, Newb.*)*, and valley oak (*Quercus lobata*, Nee), with evidence of some extent of hybridization between species (Nixon, 2002). While oaks are largely on the PFS, grasses are across the study site and include species from both native and non-native genera, including *Avena*, *Bromus*, and *Elymus* (Pers. Comm. land steward Zachariah Tuthill).

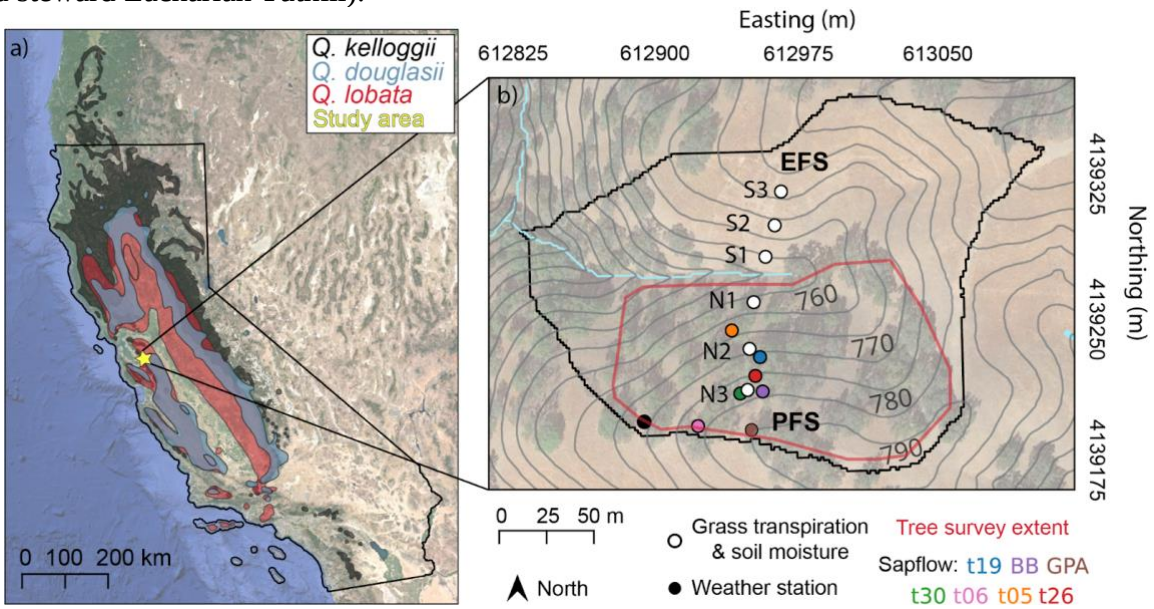

Figure 1. (a) Location of study area (yellow star) and approximate natural range of *Q. kelloggii* (black shaded region), *Q. lobata* (red shaded region), *Q. douglasii* (blue shaded region) (United States. Forest Service, 1971). Background is a Google Earth Imagery shaded relief of topography. (b) Study site with instrumentation nests of grass transpiration and soil moisture measurements (white), weather station (black), study trees with sap flow sensors (colors) and tree survey extent (red line). Stream channels are delineated in light blue; contour interval is 5 m and numbers refer to elevation in m above sea level.

2.2 Field-based transpiration measurements

We measured plot-scale, surface ET with an open-path, infrared gas analyzer (model LI-7500, LICOR, Lincoln, Nebraska) within a chamber (0.5 m x 0.5 m x 0.5 m) constructed of a PVC pipe frame, covered by Tefzel film with a fan placed inside for chamber mixing (Supplementary Figure 1; Huxman et al., 2004). This measurement included both evaporation from the ground surface and grass transpiration, however, we assume that the evaporative flux is negligible, thus we refer to this measurement as "grass transpiration" throughout the manuscript (Arnone & Obrist, 2003; Schlesinger & Jasechko, 2014). We collected measurements weekly at each instrument nest starting when the grass became active after the first rainfall (December 10, 2020) to when the grass senescence (June 10, 2021), which represented a full grass growing season. We averaged grass transpiration across landscape positions on the PFS and EFS to determine hillslope-averaged grass transpiration for each measurement period. To determine a

weekly hillslope-averaged grass transpiration, we assumed each measurement to be representative of the week and multiplied by 7 (number of days in the week). To calculate total grass growing season transpiration (December - June), we summed each hillslope-averaged grass transpiration value.

To quantify oak water use, we installed heat pulse velocity sap flow probes (Edaphic Scientific; Forster, 2019, 2020) within seven mature oak trees at 1.4 m height above ground surface (e.g., breast height) along the PFS of Arbor Creek Experimental Catchment. We chose the instrumented oak trees to include a wide range of landscape positions and sizes (Supplementary Table 1). We measured sap flux during the oak tree growing season at 10 mm (outer position) and 20 mm (inner position) within the xylem every 15-min from May - December 2021. To correct for probe misalignment during installation, we assumed zero flow after leaf off (late December 2021) and used a wound correction diameter of 0.2 mm (Burgess et al., 2001). To measure sapwood thickness, we extracted tree cores using an increment borer in August 2021 and identified a shift from translucence to opaqueness, which represented the sapwood to heartwood transition (Quiñonez-Piñón & Valeo, 2018). With these cores, we quantified wood water content and density, which we used to convert heat pulse velocity to sap flux (Burgess et al., 2001). We quantified the radial profile of sap flux in two ways and for the final calculations we assume a constant sap flux across the sapwood (see Supplementary Section 1.2 for details;(Percy Link, Kevin Simonin, Holly Maness, Jasper Oshun, Todd Dawson, Inez Fung, 2014)). To calculate sap flow volumetrically, we multiplied the sap flux by the corresponding sapwood area of the tree.

To scale oak tree sap flow measurements to hillslope-scale transpiration, we performed cruising surveys of every oak on the pole-facing hillslope (red outline in Figure 1b). A total of 113 trees were surveyed within the 12,550 m^2 survey area, which were used to estimate total hillslope-scale oak transpiration. We recorded the species and diameter at breast height (DBH) for each tree (Supplementary Table 2). Trees that forked below breast height were recorded as two individual trees. We estimated the growing season total sap flow for the surveyed trees using a power law function relating tree diameter to the growing season total sap flow for the instrumented trees. We summed the total sap flow for all trees and divided it by the survey area to quantify a hillslope-scale transpiration magnitude [mm].

2.3 Remotely-sensed NDVI and ET

To explore temporal variability in vegetation greenness, we used Google Earth Engine to extract weekly NDVI values from the mid-slope position on the PFS and EFS using images collected from January 2017 to December 2021 on the Copernicus Sentinel-2 mission (10-m spatial resolution). NDVI compares the intensity of reflectance in the visible red and near-infrared spectrum to quantify vegetation greenness (Acker et al., 2014).

We quantified ET at the mid-slope position of our study hillslopes, with remotely-sensed ET products using Python application programming interface to access models from OpenET (Melton et al., 2022). OpenET uses Landsat imagery to estimate monthly ET at 30 m resolution with a variety of approaches, including surface energy balance, Priestley-Taylor, and psychrometry (FAO, 2023)(see Supplementary 1.3 for details). A multi-model Ensemble ET estimate was calculated by OpenET based on the arithmetic average after removing outliers using the Median Absolute Deviation method (Leys et al., 2013; Volk et al., 2024). While we included the ET results from all models in the Supplementary information (Supplementary Figure 3), we used the Ensemble model for analyses in this study.

2.4 Subsurface water storage deficit calculations

We calculated the hillslope-average soil water storage [mm] by integrating soil water content from the surface to the 50 cm depth. We calculated the soil water storage deficit by subtracting the volumetric water content at each timestep from the maximum recorded volumetric water content, assuming the maximum represents a maximum unsaturated water content at field capacity. In addition, we compare this to an estimated subsurface water storage deficit calculated by the total field-based ET measurements on the EFS and the PFS.

Previous studies have shown that oak tree roots can extend beneath the soil, into the weathered bedrock, to extract deeper water storage referred to as rock moisture (Hahm et al., 2020, 2022; McCormick et al., 2021). To estimate this deeper storage we calculated the total subsurface water storage deficit (i.e. soil and rock moisture) across multiple water years, we calculated the root-zone storage deficit from October 2017 to September 2021 using statistically interpolated precipitation data (Oregon State's PRISM daily precipitation) and remotely-sensed ET (Ensemble model from OpenET; described above) following the method by (Wang-Erlandsson et al., 2016) and adapted by (Dralle et al., 2021). The method used a mass-balance approach to estimate a root-zone storage deficit as a running, integrated difference between fluxes entering and exiting the root zone, assumed to be precipitation and ET, respectively. Here, we estimated the root-zone storage deficit over subsequent water years (2017-2021), where the running deficit represents a lower-bound on the amount of ET supplied from the root zone that has not been replenished by precipitation. Therefore, the root-zone storage deficit represents the minimum amount of vegetation water uptake that is not accounted for by precipitation (refer to Wang-Erlandsson et al., 2016; Dralle et al., 2021; and McCormick et al., 2021 for details).

3 Results

3.1 Field-based estimates of grass and oak transpiration

The EFS consistently had higher weekly grass transpiration than the PFS (Figure 2). The average grass transpiration on the EFS was 3.7 mm/week, while the average on the PFS was 1.9 mm/week. The total growing season grass transpiration was 99 mm and 50 mm, on the EFS and PFS, respectively. Anecdotally, we observed higher grass density on the EFS compared to the PFS (Supplementary Figure 2).

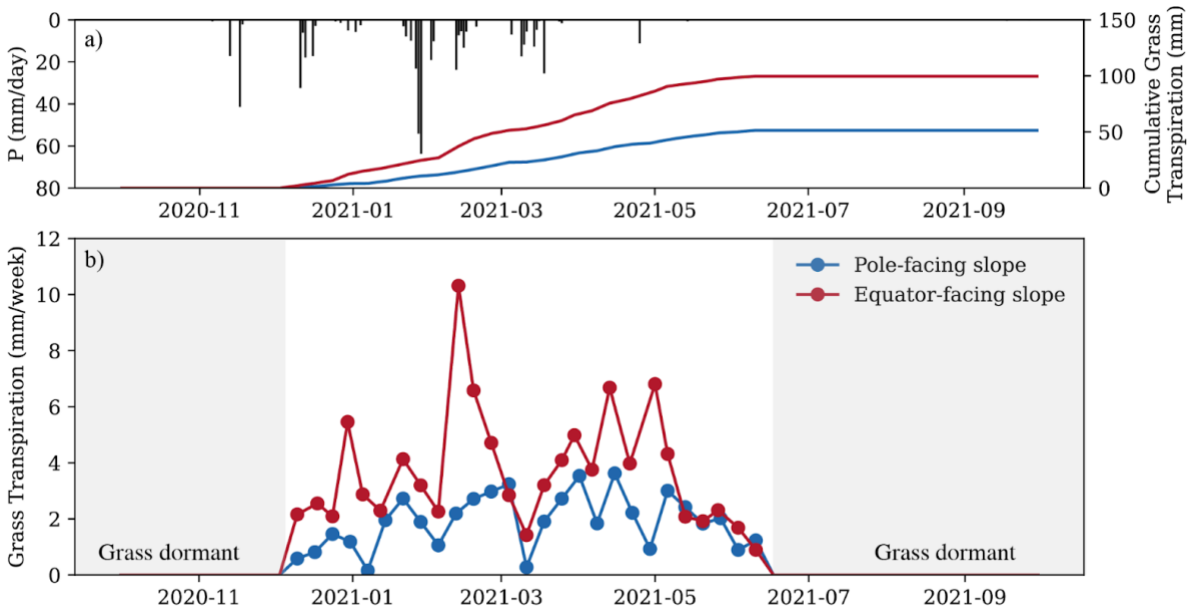

Figure 2. a) Daily precipitation (black) and cumulative grass transpiration for PFS (blue) and EFS (red) slopes, b) Slope-averaged weekly grass transpiration measurements for the PFS (blue) and EFS (red) slopes. Shaded regions are time periods with no measurements because grasses were dormant.

Oak tree transpiration varied across the growing season (Figure 3a). Oak tree leaf development began in April (not entirely recorded due to sensor installation) and transpiration was generally low until a rapid increase in May. Transpiration reached a maximum in June and remained relatively constant until late August/September, when there was a decline. In October, there was an increase in transpiration that coincided with the first precipitation event of the fall, which lasted until December when the oak trees went dormant (Figure 3a).

Average volumetric oak tree transpiration (L/day) was positively correlated with DBH (Figure 3). For example, during oak tree peak water use (June), transpiration varied by DBH from approximately 12 L/day (T30; DBH: 30.6 cm) to 1100 L/day (GPA; DBH: 108.3; Figure 3a). Consequently, total oak tree growing season transpiration generally varied with DBH (Figure 3b). From the smallest tree to the largest tree, the total growing season transpiration magnitude increased from 1427 L, 13433 L, 4373 L, 5078 L, 12988 L, 57962 L, and 147387 L (Figure 3b). The total hillslope-scale oak tree transpiration for the entire sap flow measurement period (May - December 2021) was 172 mm and 148 mm for the 2021 water year (May - September 2021).

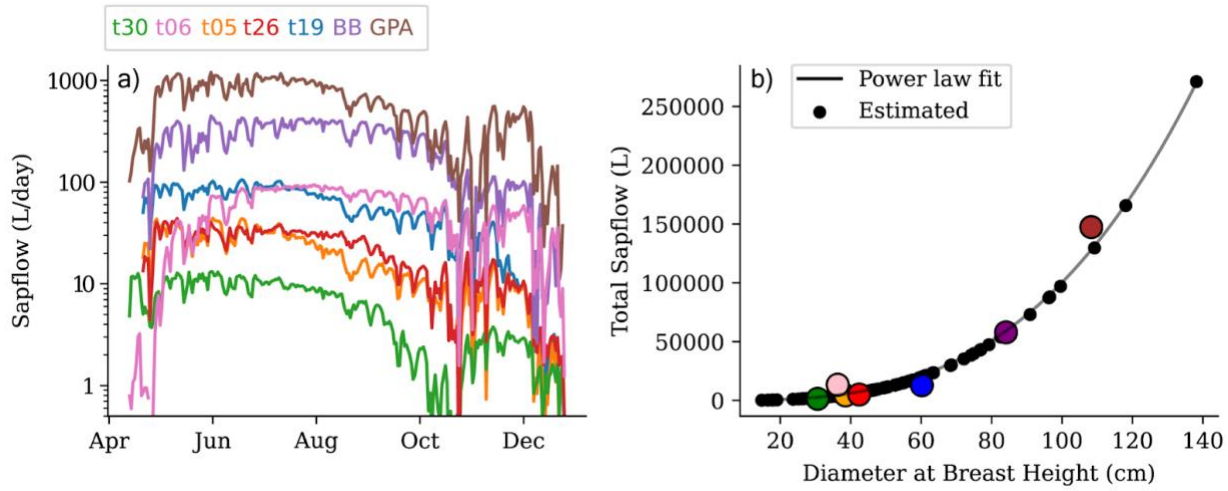

Figure 3. (a) Daily sap flow (L/day) on log-scale, (b) total sap flow (L) by DBH (cm) for each instrumented tree (colors) and surveyed trees fitted with a power-law function (black line).

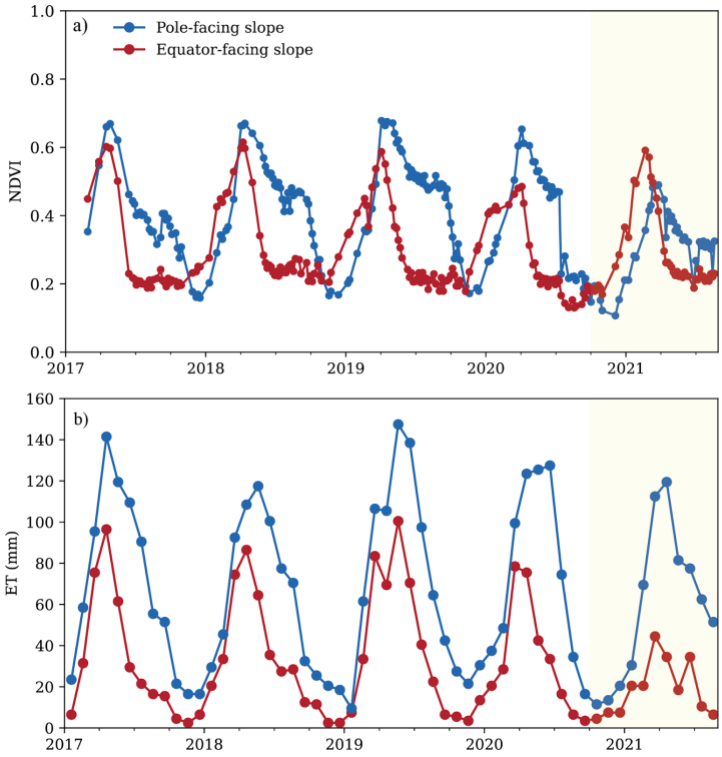

Figure 4. (a) Weekly NDVI on PFS (blue) and EFS (red) from January 2017 - September 2021. (b) Ensemble monthly ET on the PFS (blue) and EFS (red) for the same period. Timeframe of the field-based ET and soil moisture measurements are shaded in yellow.

3.2 Remotely-sensed NDVI and ET

There were annually consistent seasonal differences in NDVI values between the PFS and EFS (Figure 4a). During the winter season with only grasses actively transpiring (November - April), the EFS NDVI was on average 0.37, while the PFS NDVI was on average 0.32. During the oak tree growing season (April - October), the PFS had higher NDVI than the EFS with 0.39

and 0.28, respectively. During the 2021 water year, which coincided with our field-based measurement time period, the average NDVI values on the PFS and EFS were 0.33 and 0.28, respectively.

The remotely-sensed monthly ET was always higher on the PFS than the EFS (Figure 4b). During the winter, the average ET on the PFS was 41 mm/month, while the average ET on the EFS was 21 mm/month. During the oak tree growing season, the average ET on the PFS was 64 mm/month, while the average ET on the EFS was 29 mm/month. During the 2021 water year, the total ET on the PFS and EFS were 649 mm and 195 mm, respectively.

3.3 Subsurface water storage deficit

During the 2021 water year, the timing and magnitude of field-calculated soil water storage depletion varied by season between hillslopes with opposing aspects (Figure 5b). There was higher subsurface water storage depletion on the EFS during the winter season, when grasses were active (January - April, Figure 2). In contrast, during the summer, the EFS had negligible soil water depletion, while there was considerable soil water storage depletion on the PFS with active oak trees (Figure 5b). At the end of the summer (September), there was a slightly lower cumulative soil water storage deficit on the EFS (94 mm) than the PFS (104 mm). In comparison, field-based ET measurements for the 2021 water year (October 2020 - September 2021) were used to calculate a subsurface storage deficit of 99 mm on the EFS (i.e. total grass transpiration) and 198 mm on the PFS (i.e. total grass and oak tree transpiration).

Across the 2017 - 2021 water years, the remotely-sensed root-zone storage deficits between the PFS and EFS showed contrasting behavior. Despite variability in precipitation magnitude, the root-zone storage deficit on the EFS (average 110 mm; standard deviation = 84 mm) was replenished each year (i.e. returned to zero; Figure 6). In contrast, on the PFS, the root-zone storage deficit was not annually replenished and increased from 534 mm at the end of water year 2017 to 1608 mm at the end of water year 2021.

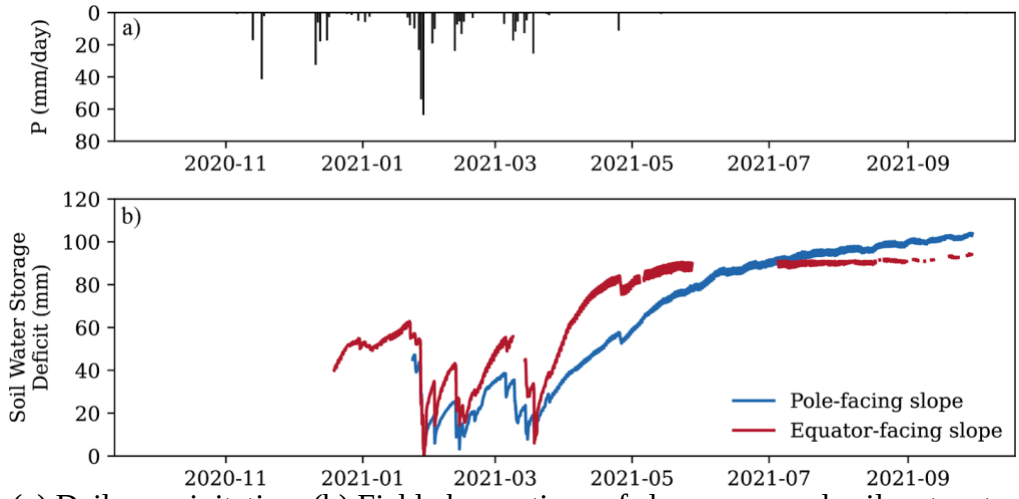

Figure 5. (a) Daily precipitation, (b) Field observations of slope-averaged soil water storage deficit within the top 50 cm from January - September 2021 on the PFS (blue) and EFS (red).

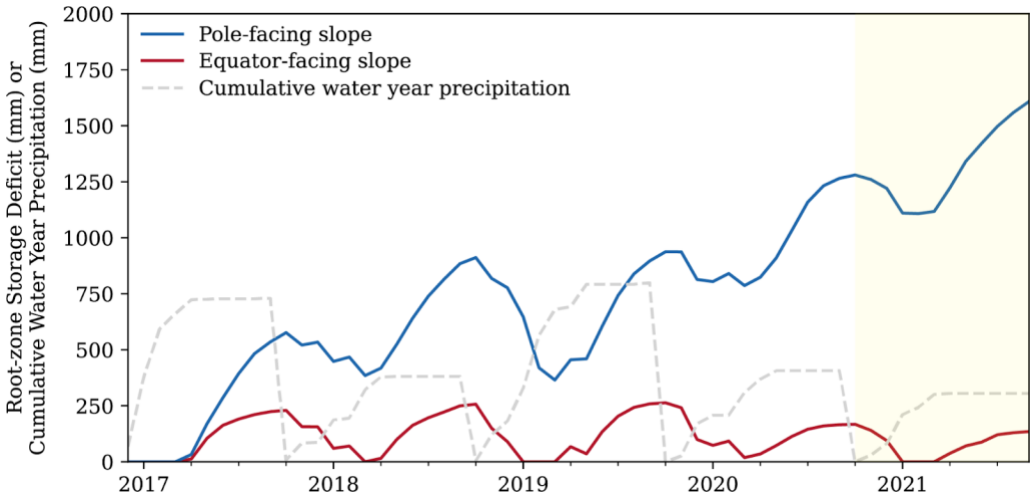

Figure 6. Monthly root-zone storage deficit for PFS (blue) and EFS (red) and cumulative water year precipitation (dashed gray) at the study site from remotely-sensed observations. The period of field-based ET and soil moisture measurements are shaded in yellow.

4 Discussion

4.1 Oak and grass transpiration in rain-dominated mediterranean climates

During water year 2021 (October 1 - September 30) the average ET within Arbor Creek Experimental Catchment ranged between 124 mm (field-based measurements) and 422 mm (remotely-sensed measurements). We interpret this range to represent a possible lower and upper bound on ET (see Section 4.3), which encompasses other reported ET values in California oak woodlands (Baldocchi et al., 2021; Lewis et al., 2000; Ma et al., 2020). Regardless of method, the majority of ET contributions were from the oak tree dominated PFS.

Extensive research quantifying and partitioning ET between oak and grass water use has been done within the Sierra Nevada, CA foothills dominated by blue oaks. For example, (Lewis et al., 2000) estimated an annual average ET of 364 mm over a 17 year period using a water balance approach. Over a similar time period, Baldocchi et al. (2021) used eddy flux towers to show that evaporative fluxes were higher within an oak savanna (420 ± 58.2 mm), compared to a nearby annual grassland (315 ± 37.7 mm). Building on this work, (Ma et al., 2020) combined nested eddy flux towers and partitioning models to determine that within the oak savanna, oak and grass transpiration contributed approximately 281 mm and 67 mm, respectively. These studies demonstrate the range of ET in oak savannas and highlight the need for more research across different environmental conditions to identify the mechanistic controls on oak water use.

Outside of the Sierra foothills, there has been limited research quantifying oak woodland ET and the role of ET on subsurface water storage deficits. A notable exception includes work by (Hahm et al., 2022) that investigated blue oak transpiration and vadose zone storage dynamics within northern California. They reported that the mean annual ET at this site was 332 mm between 2001 and 2018 (Breathing Earth System Simulator; Ryu et al., 2011). By combining sapflow sensors and borehole hydrologic monitoring, they demonstrated that oak water use during the dry growing season was sustained by rock moisture below the soil (Hahm et al., 2022). However, while the authors describe the landscape as “aspect-regulated with negligible woody-vegetation on EFS,” the authors do not include information about the differences in oak and grass water uptake that drive subsurface water storage depletion.

In alignment with this study, our field-based and remotely-sensed estimates of ET suggest that soil water storage is insufficient to sustain oak tree transpiration during the summer. In addition, previous studies within Arbor Creek Experimental Catchment have shown that groundwater during the summer is depleted below 5 m (Donaldson et al., 2023), suggesting that oak transpiration is likely reliant on rock moisture on the PFS. Therefore, our research contributes to a growing body of literature that demonstrates the ecohydrologic importance of rock moisture for oak tree health.

4.2 Ecohydrologic implications for higher ET on PFS

The magnitude and timing of vegetation water uptake exerts a strong control on subsurface water storage and movement (Li et al., 2018; Sadayappan et al., 2023). In both the field-based estimates and remotely-sensed estimates of subsurface storage deficits, we observed higher subsurface water storage deficits on PFS compared to EFS. It is likely oak tree water uptake from rock moisture may limit groundwater recharge and streamflow generation on PFS (Dralle et al., 2023). Under these conditions, we hypothesize that groundwater recharge and streamflow contributions may be higher on EFS, which is contrary to existing conceptual models of water partitioning between hillslopes with opposing aspects (Pelletier et al., 2018; Regmi et al., 2019; Webb et al., 2023). Future field work utilizing deeper measurement tools, such as a neutron probe or other geophysical tools, will be used to validate the derived estimates of subsurface water storage and test this hypothesis.

In water-limited and rain-dominated landscapes, variability in root-zone storage deficit is a strong control on the spatial distribution of ecosystem resilience to disturbances, such as drought (Callahan et al., 2022). Our results suggest that multiple consecutive years of low precipitation inputs may exacerbate root-zone water storage deficits on PFS. During multi-year droughts, consistently high root-zone storage deficits on PFS may cause oak trees to be more susceptible to mortality (Ackerly et al., 2020; Brown et al., 2018; Kueppers et al., 2005). In comparison, even in relatively low precipitation years, subsurface water storage is replenished on the EFS. This finding highlights an important question: *why aren't there oaks on the EFS with a lower subsurface water storage deficit*? We hypothesize that the absence of oak trees on EFS may be driven by higher air temperature, higher vapor pressure deficits, and lower shallow soil moisture that may limit oak seedling survival, despite potentially higher water availability below the soil (Nudurupati et al., 2023; Swiecki & Bernhardt, 1998). These findings highlight the importance of adequately representing plant functional group distributions and water uptake patterns through time to accurately refine water balances within aspect-regulated landscapes (Istanbulluoglu & Bras, 2005; Nudurupati et al., 2023; Ying et al., 2019; Zhou et al., 2013).

4.3 Multi-tool approaches to quantify oak savanna ET

An accurate quantification of hillslope-scale ET is essential for sustainable water resource management in the face of a changing climate, but it remains one of the biggest challenges within the ecohydrologic sciences (Brooks et al., 2015.; Marston et al., 2022; Ying et al., 2019). Through the advancement of field-based techniques and remote-sensing technology, the ecohydrology community is entering an exciting frontier where we can combine approaches and provide water resource managers with more accurate ET estimates (Volk et al., 2024). However, each method to quantify plant water uptake includes a suite of benefits and limitations that must be considered.

Field-based measurements using sap flow sensors can directly characterize biologically mediated plant-water uptake across diverse environmental conditions (Poyatos et al., 2021). In addition, sap flow sensors can provide high temporal resolution (e.g., minutes) data, which allows for a more robust characterization of transpiration patterns compared to remote sensing, which typically reports ET on daily to monthly time intervals (Melton et al., 2022; Link et al., 2014). However, sap flow measurements often produce a conservative estimate of ET and can be time consuming, expensive, limited in scope, and require substantial field expertise (Köstner et al., 1998). For example, re-installations early in the growing season due to probe misalignment hindered our ability to quantify transpiration in April 2021, which suggests our hillslope-scale transpiration values are underestimates. In addition, the relationship between DBH and sap flow may vary across stand structure (e.g. density, species, age) and the relationship between sapwood area and DBH may vary across the oak genus (Forrester et al., 2022; Schoppach et al., 2021, 2023). This highlights the importance of well-thought-out field-based studies to identify how stand structure influences sap flow to better constrain oak transpiration from the individual tree to hillslope-scale.

Remotely-sensed estimates of ET come with their own unique set of benefits and limitations (FAO, 2023). On the one hand, remotely-sensed ET data provides information at large spatial-scales, takes minimal time for a user to acquire, and is readily comparable between diverse landscapes and different ET models (Melton et al., 2022). On the other hand, individual ET models have known, difficult-to-resolve biases that inhibit their use within upland landscapes (Wang et al., 2022; Zhao & Li, 2015). For example, most remotely-sensed models within the OpenET ensemble do not include a correction for complex terrain (e.g., slope, aspect). The ET models' inability to correct for aspect-driven differences in solar radiation may contribute to the unexpected higher ET during the winter on the PFS despite higher field-based ET on the EFS (https://openetdata.org/known-issues/; last accessed Jan 9, 2023). Therefore, we interpreted the ensemble ET to represent an upper bound of ET and highlight the need for more remotely-sensed ET models to incorporate corrections for variable terrain indices (e.g., slope, aspect) and vegetation phenology. Given that each approach has its limitations and produces a range of ET values, a more holistic and accurate approach to quantifying ET dynamics should include multiple methods in tandem.

5 Conclusions

A commonly used conceptual model of ET, hydrologic partitioning, and landscape evolution between hillslopes with opposing aspects is based on landscapes with similar plant functional groups (e.g., trees)(Pelletier et al., 2018; Riebe et al., 2017). This conceptual model assumes that a larger energy input on EFS will induce a higher evaporative demand, increase transpiration rates, and drive higher annual ET on EFS compared to PFS (Pelletier et al., 2018). However, these studies do not account for the potential confounding influence of distinct vegetation communities on hillslopes with opposing aspects. In the Arbor Creek Experimental Catchment, we observed that our PFS had higher annual ET due to oak tree water uptake, compared to the equator-facing hillslope with only grasses. Higher ET on PFS contributed to higher subsurface water storage deficits through time. Our work reveals the importance of accurately representing vegetation types and phenology at the scale of individual hillslopes to better estimate ET and subsurface hydrologic partitioning.

Acknowledgments

The authors would like to acknowledge the financial support provided by the Betty and Gordon Moore Foundation under the project title: The California Heartbeat Initiative, National Science Foundation CAREER Grant (Award 2046957), and the Mildred E. Mathias Graduate Student Research Grant by the University of California Natural Reserve System. In addition, the authors would like to acknowledge the financial support granted by the University of California, Santa Cruz through the Kathryn D. Sullivan Impact Award and the Hammett Fellowship. The authors thank past and present members of the UC Santa Cruz Watershed Hydrology Lab, namely, Chris Causbrook, Peter Willits, Michael Wilshire, Mia Alonso, and Lauren Giggy for support in the lab and field. Thank you to Zachary Harlow and Zachariah Tuthill for land access. Todd Dawson, Kerri Johnson, Jim Norris, and Collin Bode provided thoughtful guidance and key technical assistance throughout the project. Thank you to Michael Forster for his invaluable assistance with the sap flow sensors and to the OpenET team, namely Will Carrara, for dependable technical support.

Open Research

All data used in the publication are cited in the references and are hosted on the Consortium of Universities for the Advancement of Hydrologic Science, Inc. web-based hydrologic information system(Hydroshare).http://www.hydroshare.org/resource/b10b7c5b64c246308524238586e2fb9b

References

Acker, J., Williams, R., Chiu, L., Ardanuy, P., Miller, S., Schueler, C., Vachon, P. W., & Manore, M. (2014). Remote sensing from satellites☆. *Reference Module in Earth Systems and Environmental Sciences*. https://cir.nii.ac.jp/crid/1360576123088102400

Ackerly, D. D., Kling, M. M., Clark, M. L., Papper, P., Oldfather, M. F., Flint, A. L., & Flint, L. E. (2020). Topoclimates, refugia, and biotic responses to climate change. *Frontiers in Ecology and the Environment*, *18*(5), 288–297.

Armesto, J. J., & Martínez, J. A. (1978). Relations Between Vegetation Structure and Slope Aspect in the Mediterranean Region of Chile. *The Journal of Ecology*, *66*(3), 881–889.

Arnone, J. A., & Obrist, D. (2003). A large daylight geodesic dome for quantification of whole-ecosystem CO2 and water vapour fluxes in arid shrublands. *Journal of Arid Environments*, *55*(4), 629–643.

436 Baldocchi, D., Chen, Q., Chen, X., Ma, S., Miller, G., Ryu, Y., Xiao, J., Wenk, R., Battles, J., &
437 Taylor, C. (n.d.). *The dynamics of energy, water and carbon fluxes in a blue oak (Quercus*
438 *douglasii) Savanna in California, USA*. Retrieved January 8, 2024, from
439 https://nature.berkeley.edu/biometlab/pdf/Flux%20dynamics%20in%20a%20blue%20oak%2
440 0savanna%20in%20California%20revised.pdf
441 Baldocchi, D., Ma, S., & Verfaillie, J. (2021). On the inter- and intra-annual variability of
442 ecosystem evapotranspiration and water use efficiency of an oak savanna and annual
443 grassland subjected to booms and busts in rainfall. *Global Change Biology*, *27*(2), 359–375.
444 Bilir, T. E., Fung, I., & Dawson, T. E. (2021). Slope-aspect induced climate differences influence
445 how water is exchanged between the land and atmosphere. *Journal of Geophysical Research.*
446 *Biogeosciences*, *126*(5). https://doi.org/10.1029/2020jg006027
447 Brooks, P. D., Chorover, J., & Fan, Y. (2015). Hydrological partitioning in the critical zone:
448 Recent advances and opportunities for developing transferable understanding of water cycle
449 dynamics. *Water Resources*. https://doi.org/10.1002/2015WR017039
450 Brown, B. J., McLaughlin, B. C., Blakey, R. V., & Morueta-Holme, N. (2018). Future
451 vulnerability mapping based on response to extreme climate events: Dieback thresholds in an
452 endemic California oak. *Diversity & Distributions*, *24*(9), 1186–1198.
453 Burgess, S. S., Adams, M. A., Turner, N. C., Beverly, C. R., Ong, C. K., Khan, A. A., & Bleby, T.
454 M. (2001). An improved heat pulse method to measure low and reverse rates of sap flow in
455 woody plants. *Tree Physiology*, *21*(9), 589–598.
456 Burns, E. F., Rempe, D. M., Parsekian, A. D., Schmidt, L. M., Singha, K., & Barnard, H. R.
457 (2023). Ecohydrologic dynamics of rock moisture in a Montane catchment of the Colorado
458 front range. *Water Resources Research*, *59*(6). https://doi.org/10.1029/2022wr034117

459 Callahan, R. P., Riebe, C. S., Sklar, L. S., Pasquet, S., Ferrier, K. L., Hahm, W. J., Taylor, N. J.,
460 Grana, D., Flinchum, B. A., Hayes, J. L., & Holbrook, W. S. (2022). Forest vulnerability to
461 drought controlled by bedrock composition. *Nature Geoscience*, *15*(9), 714–719.
462 Chorover, J., Troch, P. A., Rasmussen, C., Brooks, P. D., Pelletier, J. D., Breshears, D. D.,
463 Huxman, T. E., Kurc, S. A., Lohse, K. A., McIntosh, J. C., Meixner, T., Schaap, M. G.,
464 Litvak, M. E., Perdrial, J., Harpold, A., & Durcik, M. (2011). How water, carbon, and energy
465 drive critical zone evolution: The jemez–Santa Catalina Critical Zone Observatory. *Vadose*
466 *Zone Journal: VZJ*, *10*(3), 884–899.
467 Donaldson, A. M., Zimmer, M., Huang, M.-H., Johnson, K. N., Hudson-Rasmussen, B., Finnegan,
468 N., Barling, N., & Callahan, R. P. (2023). Symmetry in hillslope steepness and saprolite
469 thickness between hillslopes with opposing aspects. *Journal of Geophysical Research. Earth*
470 *Surface*, *128*(7). https://doi.org/10.1029/2023jf007076
471 Dralle, D. N., Hahm, W. J., Chadwick, K. D., McCormick, E., & Rempe, D. M. (2021). Technical
472 note: Accounting for snow in the estimation of root zone water storage capacity from
473 precipitation and evapotranspiration fluxes. *Hydrology and Earth System Sciences*, *25*(5),
474 2861–2867.
475 Dralle, D. N., Hahm, W. J., & Rempe, D. M. (2023). Inferring hillslope groundwater recharge
476 ratios from the storage-discharge relation. *Geophysical Research Letters*, *50*(14).
477 https://doi.org/10.1029/2023gl104255
478 FAO. (2023). *Remote sensing determination of evapotranspiration – Algorithms, strengths,*
479 *weaknesses, uncertainty and best fit-for-purpose*. FAO. https://doi.org/10.4060/cc8150en

480 Forrester, D. I., Limousin, J.-M., & Pfautsch, S. (2022). The relationship between tree size and tree
481 water-use: is competition for water size-symmetric or size-asymmetric? *Tree Physiology*,
482 *42*(10), 1916–1927.
483 Forster, M. A. (2019). The Dual Method Approach (DMA) Resolves Measurement Range
484 Limitations of Heat Pulse Velocity Sap Flow Sensors. *Forests, Trees and Livelihoods*, *10*(1),
485 46.
486 Forster, M. A. (2020). The importance of conduction versus convection in heat pulse sap flow
487 methods. *Tree Physiology*, *40*(5), 683–694.
488 García-Gamero, V., Peña, A., Laguna, A. M., Giráldez, J. V., & Vanwalleghem, T. (2021). Factors
489 controlling the asymmetry of soil moisture and vegetation dynamics in a hilly Mediterranean
490 catchment. *Journal of Hydrology*, *598*, 126207.
491 Gutiérrez-Jurado, H. A., Vivoni, E. R., Cikoski, C., Harrison, J. B. J., Bras, R. L., &
492 Istanbulluoglu, E. (2013). On the observed ecohydrologic dynamics of a semiarid basin with
493 aspect-delimited ecosystems. *Water Resources Research*, *49*(12), 8263–8284.
494 Hahm, W. J., Dralle, D. N., Sanders, M., Bryk, A. B., Fauria, K. E., Huang, M. H., Hudson-
495 Rasmussen, B., Nelson, M. D., Pedrazas, M. A., Schmidt, L., Whiting, J., Dietrich, W. E., &
496 Rempe, D. M. (2022). Bedrock vadose zone storage dynamics under extreme drought:
497 Consequences for plant water availability, recharge, and runoff. *Water Resources Research*,
498 *58*(4). https://doi.org/10.1029/2021wr031781
499 Hahm, W. J., Rempe, D. M., Dralle, D. N., Dawson, T. E., & Dietrich, W. E. (2020). Oak
500 transpiration drawn from the weathered bedrock vadose zone in the summer dry season.
501 *Water Resources Research*, *56*(11). https://doi.org/10.1029/2020wr027419

Hassler, S. K., Weiler, M., & Blume, T. (2018). Tree-, stand- and site-specific controls on landscape-scale patterns of transpiration. *Hydrology and Earth System Sciences*, *22*(1), 13–30.

Holst, J., Grote, R., Offermann, C., Ferrio, J. P., Gessler, A., Mayer, H., & Rennenberg, H. (2010). Water fluxes within beech stands in complex terrain. *International Journal of Biometeorology*, *54*(1), 23–36.

Huxman, T. E., Cable, J. M., Ignace, D. D., Eilts, J. A., English, N. B., Weltzin, J., & Williams, D. G. (2004). Response of net ecosystem gas exchange to a simulated precipitation pulse in a semi-arid grassland: the role of native versus non-native grasses and soil texture. *Oecologia*, *141*(2), 295–305.

Istanbulluoglu, E., & Bras, R. L. (2005). Vegetation-modulated landscape evolution: Effects of vegetation on landscape processes, drainage density, and topography. *Journal of Geophysical Research*, *110*(F2). https://doi.org/10.1029/2004jf000249

Köstner, B., Granier, A., & Cermák, J. (1998). Sapflow measurements in forest stands: methods and uncertainties. *Annales Des Sciences Forestières*, *55*(1-2), 13–27.

Kueppers, L. M., Snyder, M. A., Sloan, L. C., Zavaleta, E. S., & Fulfrost, B. (2005). Modeled regional climate change and California endemic oak ranges. *Proceedings of the National Academy of Sciences of the United States of America*, *102*(45), 16281–16286.

Kumari, N., Saco, P. M., Rodriguez, J. F., Johnstone, S. A., Srivastava, A., Chun, K. P., & Yetemen, O. (2020). The grass is not always greener on the other side: Seasonal reversal of vegetation greenness in aspect-driven semiarid ecosystems. *Geophysical Research Letters*, *47*(15). https://doi.org/10.1029/2020gl088918

Lewis, D., Singer, M. J., Dahlgren, R. A., & Tate, K. W. (2000). Hydrology in a California oak woodland watershed: a 17-year study. *Journal of Hydrology*, *240*(1), 106–117.

Leys, C., Ley, C., Klein, O., Bernard, P., & Licata, L. (2013). Detecting outliers: Do not use standard deviation around the mean, use absolute deviation around the median. *Journal of Experimental Social Psychology*, *49*(4), 764–766.

Li, H., Si, B., & Li, M. (2018). Rooting depth controls potential groundwater recharge on hillslopes. *Journal of Hydrology*, *564*, 164–174.

Marston, L. T., Abdallah, A. M., Bagstad, K. J., Dickson, K., Glynn, P., Larsen, S. G., Melton, F. S., Onda, K., Painter, J. A., Prairie, J., Ruddell, B. L., Rushforth, R. R., Senay, G. B., & Shaffer, K. (2022). Water-use data in the United States: Challenges and future directions. *Journal of the American Water Resources Association*, *58*(4), 485–495.

Ma, S., Eichelmann, E., Wolf, S., Rey-Sanchez, C., & Baldocchi, D. D. (2020). Transpiration and evaporation in a Californian oak-grass savanna: Field measurements and partitioning model results. *Agricultural and Forest Meteorology*, *295*, 108204.

McCormick, E. L., Dralle, D. N., Hahm, W. J., Tune, A. K., Schmidt, L. M., Chadwick, K. D., & Rempe, D. M. (2021). Widespread woody plant use of water stored in bedrock. *Nature*, *597*(7875), 225–229.

Melton, F. S., Huntington, J., Grimm, R., Herring, J., Hall, M., Rollison, D., Erickson, T., Allen, R., Anderson, M., Fisher, J. B., Kilic, A., Senay, G. B., Volk, J., Hain, C., Johnson, L., Ruhoff, A., Blankenau, P., Bromley, M., Carrara, W., … Anderson, R. G. (2022). OpenET: Filling a critical data gap in water management for the western United States. *Journal of the American Water Resources Association*, *58*(6), 971–994.

546 Nixon, K. C. (2002). The oak (Quercus) biodiversity of California and adjacent regions. *USDA*
547 *Forest Service General Technical Report PSW*.
548 https://www.researchgate.net/profile/William_Tietje/publication/237372538_Cavity-
549 nesting_Bird_Use_of_Nest_Boxes_in_Vineyards_of_Central-
550 Coast_California1/links/640d142166f8522c38997b15/Cavity-nesting-Bird-Use-of-Nest-
551 Boxes-in-Vineyards-of-Central-Coast-California1.pdf#page=13
552 Nudurupati, S. S., Istanbulluoglu, E., Tucker, G. E., Gasparini, N. M., Hobley, D. E. J., Hutton, E.
553 W. H., Barnhart, K. R., & Adams, J. M. (2023). On transient semi-arid ecosystem dynamics
554 using Landlab: Vegetation shifts, topographic Refugia, and response to climate. *Water*
555 *Resources Research*, *59*(4). https://doi.org/10.1029/2021wr031179
556 Pelletier, J. D., Barron-Gafford, G. A., Gutiérrez-Jurado, H., Hinckley, E.-L. S., Istanbulluoglu, E.,
557 McGuire, L. A., Niu, G.-Y., Poulos, M. J., Rasmussen, C., Richardson, P., Swetnam, T. L., &
558 Tucker, G. E. (2018). Which way do you lean? Using slope aspect variations to understand
559 Critical Zone processes and feedbacks. *Earth Surface Processes and Landforms*, *43*(5),
560 1133–1154.
561 Percy Link, Kevin Simonin, Holly Maness, Jasper Oshun, Todd Dawson, Inez Fung. (2014).
562 Species differences in the seasonality of evergreen tree transpiration in a Mediterranean
563 climate: Analysis of multiyear, half-hourly sap flow observations. *Water Resources*.
564 https://doi.org/10.1002/2013WR014023
565 Poyatos, R., Werner, C., & Martínez-Vilalta, J. (2021). *Global Transpiration Data from Sap Flow*
566 *Measurements: the SAPFLUXNET Database*. Universität.

Quiñonez-Piñón, M. R., & Valeo, C. (2018). Assessing the Translucence and Color-Change Methods for Estimating Sapwood Depth in Three Boreal Species. *Forests, Trees and Livelihoods*, *9*(11), 686.

Regmi, N. R., McDonald, E. V., & Rasmussen, C. (2019). Hillslope response under variable microclimate. *Earth Surface Processes and Landforms*, *44*(13), 2615–2627.

Riebe, C. S., Hahm, W. J., & Brantley, S. L. (2017). Controls on deep critical zone architecture: a historical review and four testable hypotheses. *Earth Surface Processes and Landforms*, *42*(1), 128–156.

Ryu, Y., Baldocchi, D. D., Kobayashi, H., van Ingen, C., Li, J., Black, T. A., Beringer, J., van Gorsel, E., Knohl, A., Law, B. E., & Roupsard, O. (2011). Integration of MODIS land and atmosphere products with a coupled-process model to estimate gross primary productivity and evapotranspiration from 1 km to global scales. *Global Biogeochemical Cycles*, *25*(4). https://doi.org/10.1029/2011gb004053

Sadayappan, K., Keen, R., Jarecke, K. M., Moreno, V., Nippert, J. B., Kirk, M. F., Sullivan, P. L., & Li, L. (2023). Drier streams despite a wetter climate in woody-encroached grasslands. *Journal of Hydrology*, *627*, 130388.

Schlesinger, W. H., & Jasechko, S. (2014). Transpiration in the global water cycle. *Agricultural and Forest Meteorology, 189-190*, 115–117.

Schoppach, R., Chun, K. P., He, Q., Fabiani, G., & Klaus, J. (2021). Species-specific control of DBH and landscape characteristics on tree-to-tree variability of sap velocity. *Agricultural and Forest Meteorology, 307*, 108533.

588 Schoppach, R., Chun, K. P., & Klaus, J. (2023). Allometric relations between DBH and sapwood
589 area for predicting stand transpiration: lessons learned from the Quercus genus. *European*
590 *Journal of Forest Research*, *142*(4), 797–809.
591 Smith, T., & Bookhagen, B. (2021). Climatic and biotic controls on topographic asymmetry at the
592 global scale. *Journal of Geophysical Research. Earth Surface*, *126*(1).
593 https://doi.org/10.1029/2020jf005692
594 Swiecki, T. J., & Bernhardt, E. (1998). Understanding blue oak regeneration. *Fremontia*, *26*(1),
595 19–26.
596 United States. Forest Service. (1971). *Atlas of United States Trees: (no.1146). Conifers and*
597 *important hardwoods, by E.L. Little, Jr*. U.S. Government Printing Office.
598 Volk, J. M., Huntington, J. L., Melton, F. S., Allen, R., Anderson, M., Fisher, J. B., Kilic, A.,
599 Ruhoff, A., Senay, G. B., Minor, B., Morton, C., Ott, T., Johnson, L., Comini de Andrade,
600 B., Carrara, W., Doherty, C. T., Dunkerly, C., Friedrichs, M., Guzman, A., … Yang, Y.
601 (2024). Assessing the accuracy of OpenET satellite-based evapotranspiration data to support
602 water resource and land management applications. *Nature Water*, 1–13.
603 Wang-Erlandsson, L., Bastiaanssen, W. G. M., Gao, H., Jägermeyr, J., Senay, G. B., van Dijk, A.
604 I. J. M., Guerschman, J. P., Keys, P. W., Gordon, L. J., & Savenije, H. H. G. (2016). Global
605 root zone storage capacity from satellite-based evaporation. *Hydrology and Earth System*
606 *Sciences*, *20*(4), 1459–1481.
607 Wang, L., Wu, B., Elnashar, A., Zhu, W., Yan, N., Ma, Z., Liu, S., & Niu, X. (2022).
608 Incorporation of Net Radiation Model Considering Complex Terrain in Evapotranspiration
609 Determination with Sentinel-2 Data. *Remote Sensing*, *14*(5), 1191.

610 Webb, R. W., Litvak, M. E., & Brooks, P. D. (2023). The role of terrain-mediated hydroclimate in
611 vegetation recovery after wildfire. *Environmental Research Letters: ERL [Web Site]*, *18*(6),
612 064036.
613 Ying, F., Martyn, C., David M., L., Sean, S., L. E., B., Brantley, S. L., Brooks, P. D., Dietrich, W.
614 E., Flores, A., Grant, G., Kirchner, J. W., D. S., M., J. J., M., Paul, M., P. L., S., C., T., H.,
615 A., N., C., A., H., … C., S. (2019). Hillslope hydrology in global change research and earth
616 system modeling. *Water Resources Research*.
617 https://agupubs.onlinelibrary.wiley.com/doi/abs/10.1029/2018wr023903
618 Zapata-Rios, X., Brooks, P. D., Troch, P. A., McIntosh, J., & Guo, Q. (2016). Influence of terrain
619 aspect on water partitioning, vegetation structure and vegetation greening in high-elevation
620 catchments in northern New Mexico. *Ecohydrology*, *9*(5), 782–795.
621 Zhao, W., & Li, A. (2015). A Review on Land Surface Processes Modelling over Complex
622 Terrain. *Advances in Meteorology*, *2015*. https://doi.org/10.1155/2015/607181
623 Zhou, X., Istanbulluoglu, E., & Vivoni, E. R. (2013). Modeling the ecohydrological role of aspect-
624 controlled radiation on tree-grass-shrub coexistence in a semiarid climate. *Water Resources*
625 *Research*, *49*(5), 2872–2895.